

RESEARCH ARTICLE

10.1002/2016JD026042

Key Points:

- Afternoon rainfall more frequent over drier patches during dry times, but more frequent over wet patches during extremely wet times
- Heterogeneity turns negative coupling more negative, and positive less positive
- Negative spatial coupling tends to enhance the soil moisture heterogeneity rather than leading to homogeneously wetter soils on the next day

Supporting Information:

- Supporting Information S1

Correspondence to:

M.-H. Lo,
minhuilo@ntu.edu.tw

Citation:

Hsu, H., M.-H. Lo, B. P. Guillod, D. G. Miralles, and S. Kumar (2017), Relation between precipitation location and antecedent/subsequent soil moisture spatial patterns, *J. Geophys. Res. Atmos.*, 122, 6319–6328, doi:10.1002/2016JD026042.

Received 2 OCT 2016

Accepted 8 JUN 2017

Accepted article online 17 JUN 2017

Published online 29 JUN 2017

Relation between precipitation location and antecedent/subsequent soil moisture spatial patterns

Hsin Hsu¹ , Min-Hui Lo¹ , Benoit P. Guillod^{2,3} , Diego G. Miralles⁴ , and Sanjiv Kumar⁵ 
¹Department of Atmospheric Sciences, National Taiwan University, Taipei, Taiwan, ²Environmental Change Institute, University of Oxford, Oxford, UK, ³Institute for Environmental Decisions and Institute for Atmospheric and Climate Science, ETH Zurich, Zurich, Switzerland, ⁴Laboratory of Hydrology and Water Management, Ghent University, Ghent, Belgium, ⁵School of Forestry and Wildlife Science, Auburn University, Auburn, Alabama, USA

Abstract Recent evidence has shown that relations between soil moisture and precipitation at spatial and temporal aspect are contrary to each other: afternoon precipitation tends to occur at times in which conditions are overall wet and heterogeneous in the morning, but preferentially over those patches that are relatively drier than the surroundings. This study expands the notion of soil moisture-precipitation spatial coupling by analyzing the preferred precipitation location over a range of different soil moisture patterns. Using global observations of precipitation and observationally constrained evaporative stress estimates, we confirm that relatively drier patches have more chances of receiving rain, but the preference is weakened under wetter soil conditions. During extremely wet times, wet patches have more chances of receiving rain. Moreover, the preference of precipitation to occur on drier soils is stronger when soil moisture conditions are heterogeneous. Such results indicate that the positive feedback mechanism becomes more positive as soil wetness increases and the negative feedback mechanism becomes more negative as soils become drier and more heterogeneous. The strength of these two feedback mechanisms jointly affects preferential precipitation location. Counterintuitively, analysis from 1 day after-event soil moisture pattern shows that negative soil moisture-precipitation coupling may in turn further heterogenize soil moisture patterns, because dry patch gets extremely wet with no or less rain in surrounding. Although results here do not necessarily imply a causal relationship, this work contributes to enhancing our understanding of soil moisture-precipitation spatial coupling and exposes the complex nuances of these land-atmosphere interactions.

1. Introduction

Processes at the interface between the land and atmosphere are a critical component in the climate system [Seneviratne et al., 2010]. The atmospheric boundary layer can be heated by the sensible heat flux and moistened by evapotranspiration from the land surface. With sufficient energy supply, soil moisture content is the primary constraint on evapotranspiration [Seneviratne et al., 2010]; thus, the spatial heterogeneity and variability of soil moisture induce feedbacks on temperature and precipitation that have long been recognized as an important driver of climate variability [Brubaker et al., 1993].

Along this importance, soil moisture is highly variable in space and time and difficult to measure accurately over large regions. Temporally, local soil moisture anomalies can influence surface albedo (and thus available energy at the surface) [e.g., Eltahir, 1998] and the partitioning of available energy into radiative versus latent and sensible components [Koster et al., 2004; Miralles et al., 2014; Zhou et al., 2016]; hence, they can further affect the frequency and magnitude of precipitation events by modifying atmospheric humidity and temperature [Eltahir and Bras, 1996; Eltahir, 1998; Findell and Eltahir, 2003; Schär et al., 1999; Dirmeyer et al., 2012]. Spatially, patterns in soil moisture on scales of tens of kilometers (i.e., mesoscale) can also modify local daytime circulations [Ookouchi et al., 1984] and thus provide additional low-level atmospheric convergence/divergence [Taylor et al., 2011]. Through its interplay with atmospheric conditions (such as the background wind pattern), the spatial distribution of soil moisture can exert some control on the preferred location for convective initiation [Froidevaux et al., 2014]. These mechanisms directly and indirectly affect the frequency, amount, and location of the water that returns to the land surface. These processes can, under certain circumstances, induce positive and negative land-atmosphere feedbacks at different temporal and spatial scales and thus play roles in water and energy cycles [Guillod et al., 2015].

Several studies have focused on identifying the feedback between soil moisture and precipitation using in situ and satellite observations. Early work based on observations from Illinois [Findell and Eltahir, 1997; D'Odorico and Porporato, 2004] and West Africa [Taylor and Lebel, 1998] indicated that soil moisture conditions are positively related to subsequent rainfall, suggesting a positive soil moisture-precipitation feedback. Studies based on reanalysis data exploring the sensitivity of precipitation to local evaporation also support the existence of an overall positive feedback [e.g., Findell et al., 2011; Berg et al., 2013]. However, using satellite data, a negative feedback was uncovered by Taylor et al. [2011] in the Sahelian region: the frequency of observed afternoon precipitation appeared enhanced over drier patches of soil on scales of tens of kilometers, as a result of soil moisture-induced mesoscale circulations. Taylor et al. [2012] subsequently found a dominant negative coupling between afternoon precipitation location and morning soil moisture for most parts of the world, highlighting the importance of mesoscale soil moisture heterogeneity for convective initiation. Ever since, other studies have also found negative feedbacks between soil moisture and precipitation in Europe [Taylor, 2015], in the Amazon during the dry season [Harper et al., 2014; Lin et al., 2016], and, under certain synoptic conditions and atmospheric forcing, also in Oklahoma [Ford et al., 2015].

Nowadays, there is a certain consensus that rainfall occurs preferably in times in which soils are wetter than their climatological expectation (i.e., consistent with positive temporal feedback), even though the extent to which this relates to the atmospheric persistency remains unclear [Guillod et al., 2014]. However, the spatial character of interactions between soil moisture and precipitation remains less understood: the roles of soil wetness and soil moisture heterogeneity on precipitation have been typically explored in isolation [Eltahir, 1998; Findell and Eltahir, 2003; Schär et al., 1999; Taylor et al., 2011, 2012]. Just recently, Guillod et al. [2015] directly compared the spatial and temporal aspects of this coupling for the first time, using remote sensing-based data sets, and found that rain tends to occur at times in which conditions are wet and heterogeneous, but preferentially over the locally drier patches. Nonetheless, the conclusion of Guillod et al. [2015] does not necessarily imply causality, in particular for the positive temporal relationship which could be caused by atmospherically driven persistence. In addition, the strength of these feedbacks and their dependency on soil moisture levels and heterogeneity, as well as the implications of subsequent precipitation events on the feedback strength, are issues that have not been assessed within an individual analysis using unified observations. The objectives of this study are to understand these aspects: to reveal how soil moisture conditions affect the sign of the spatial coupling and how the resulting precipitation events modify subsequent (1 day after-event) soil moisture heterogeneity, i.e., whether the preference for rain on drier soils tends to homogenize soil moisture spatial patterns.

2. Data and Methodology

2.1. Data

To examine the soil moisture spatial distribution before and after precipitation events, 10 years of global remotely sensed precipitation data and satellite-based evaporative stress are applied. We use three global precipitation estimates based on satellite microwave observations: the Climate Prediction Center morphing method (CMORPH) [Joyce et al., 2004], available from 60°S to 60°N; Precipitation Estimation from Remotely Sensed Information using Artificial Neural Networks (PERSIANN) [Hsu et al., 1997], available from 60°S to 60°N; and Tropical Rainfall Measuring Mission (TRMM3B42, hereafter referred to as TRMM) [Huffman et al., 2007], available from 50°S to 50°N. The three of them cover the period 2002–2011 at a high spatial ($0.25^\circ \times 0.25^\circ$) and temporal (3-hourly) resolution. To identify afternoon precipitation, the 3-hourly precipitation data were adjusted to local time based on a linear interpolation according to longitude prior to the analysis.

The evaporative stress data come from Global Land Evaporation Amsterdam Model (GLEAM) [Miralles et al., 2011; Martens et al., 2016]. GLEAM estimates daily evaporation, root zone soil moisture, and evaporative stress based on remotely sensed observations of net surface radiation, near-surface air temperature, precipitation, vegetation water content, surface soil moisture, and snow water equivalent. Despite relying on several model assumptions and being sensitive to uncertainties on its forcing and ancillary data [Martens et al., 2016], GLEAM has two main advantages for the study of land atmospheric interactions: (a) estimates of soil

moisture refer to the entire depth affecting evaporation and (b) the assimilation of soil moisture in combination with meteorological forcing improves the quality of soil moisture estimation.

Here we use the modified version of GLEAM by *Guilod et al.* [2014, 2015], which provides an estimate of morning (~09:00 local time) total evaporative stress (S), defined as $S = (E_s + E_t)/(E_{s,p} + E_{t,p})$, where E_s refers to soil evaporation, E_t to transpiration, and $E_{s,p}$ and $E_{t,p}$ to potential soil evaporation and potential transpiration (respectively). Therefore, S values range between 0 (soil moisture equal or below wilting point) and 1 (moisture content equal or above critical soil moisture). Moreover, this version of GLEAM does not include the interception loss. The version of GLEAM by *Guilod et al.* [2014, 2015] assimilates surface soil moisture from local nighttime passes (local time 1:30 A.M.) of Advanced Microwave Scanning Radiometer for EOS (AMSR-E) using the LPRM (Land Parameter Retrieval Model) algorithm [*Owe et al.*, 2008], and it is driven by surface radiation data from the Clouds and the Earth's Radiation Energy System (CERES) [*Wielicki et al.*, 1996], air temperature from ERA-Interim [*Dee et al.*, 2011], vegetation optical depth (LPRM), and each of the three precipitation data sets listed above. All these input data sets have been downsampled to 0.25° resolution using a bilinear interpolation, and variables have been aggregated to a daily cycle starting and ending at 09:00. We note that because of the difficulty to retrieve soil moisture beneath dense canopies and the errors in precipitation observations in tropical forests, the uncertainties of S over these regions are expected to be larger (discussed later). The S data sets are referred to as GLEAMc, GLEAMp, and GLEAMt, for CMORPH, PERSIANN, and TRMM (respectively). The results discussed here will be based on the use of CMORPH (i.e., GLEAMc), while analogous results from the other precipitation data sets are presented in the supporting information for comparison.

2.2. Precipitation Event Detection Methodology

To identify afternoon precipitation events, we employ the precipitation event detection method by *Taylor et al.* [2012] as modified by *Guilod et al.* [2015]. Because a clear negative soil moisture-precipitation coupling signal on scales of 50–100 km was found in previous remotely sensed data-based studies [*Taylor et al.*, 2011, 2012; *Guilod et al.*, 2015], we follow such spatial scale in this study. A precipitation event domain (denoted as L_{evt}) is defined as a 5×5 collection of grid cells ($0.25^\circ \times 0.25^\circ$ each, $1.25^\circ \times 1.25^\circ$ in total) centered at the location of a local maximum in accumulated precipitation of >4 mm (denoted as L_{max}) during the afternoon (defined as 12:00–24:00). We only preserve the event having the largest accumulated precipitation during the day for the L_{max} to prevent overlap between several events on any given day.

We also exclude events by applying the following filters. First, the event with at least one of its grid cell receives >1 mm of precipitation from 06:00 to 12:00 on the same day or from 00:00 to 12:00 on the next day is filtered from the analysis; this is done to retain only new rainfall events and to ensure that next day's soil moisture is modified by the previous afternoon precipitation only. Second, grid cell with topographic height variability exceeding 300 m (maximum height minus minimum height within the 0.25° grid cell) are not considered in the analysis; topographic data are from 0.017° ETOPO1 [*Amante and Eakins*, 2009]. Third, grid cells with water covering more than 5% of their area are also excluded; land cover information is from 1 km global land cover 2000 data set (GLC2000) [*Bartholomé and Belward*, 2005]. The mask of geomorphology filters, displayed in Figure 1a, highlights widespread areas which are thereby not considered in the analysis, a feature that should be kept in mind when interpreting the results. Additionally, we only analyze the seasons in which convective precipitation is dominant [*Yang and Smith*, 2008]: May–September over north of 23°N , November–March over south of 23°S , and all months in the tropics [*Guilod et al.*, 2015]. Figure 1b displays the number of afternoon rainfall events included in the analysis at a scale of 5° for the 10 year CMORPH data set. Results for different precipitation data sets are shown in supporting information Figure S1. The evolution of stress and precipitation in the days before and after an event are provided in supporting information Figure S2.

2.3. Soil Moisture Distribution

To describe the soil moisture conditions prior to the afternoon precipitation, we use preprecipitation maximum S at day i (the day of the event) within the L_{evt} domain as an indicator of soil wetness, hereafter referred to as $S_{\text{max}}(i)$. We use $S_{\text{max}}(i)$ instead of spatial mean S to ensure cases with overall dry conditions but few wet pixels to be characterized as wet events. Nonetheless, results using the spatial mean S to assess the

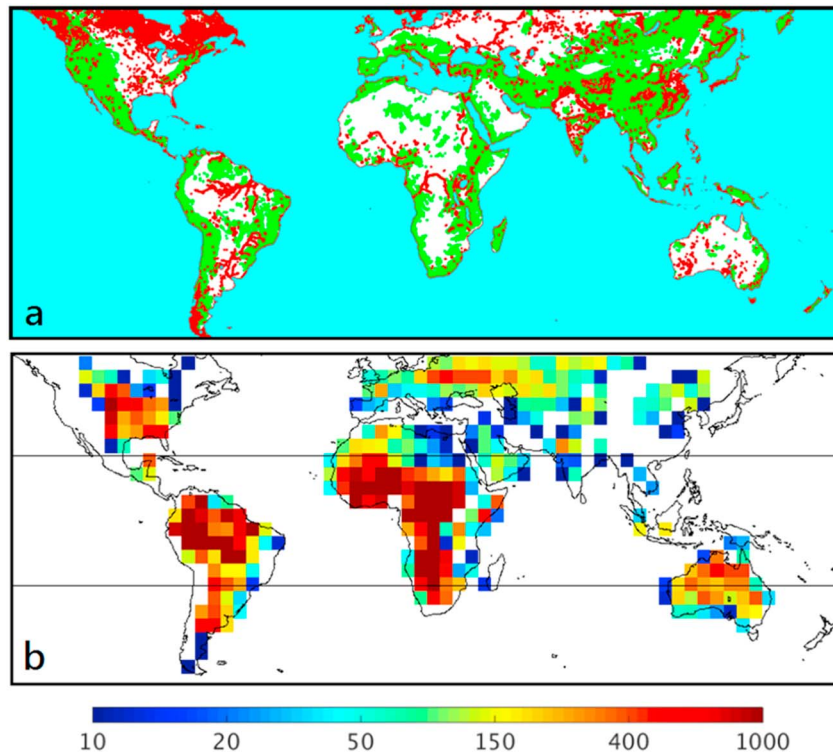


Figure 1. (a) The geomorphology filters for individual 0.25° grid used in precipitation detection method. Red: water bodies cover more than 5%; green: topography gradients ≥ 300 m. (b) Number of afternoon rain events for each 5° box for CMORPH. The latitudes with different analyzed months are divided by horizontal black lines.

relationship are also discussed in section 4 and supporting information figures. Soil moisture heterogeneity prior to the event—hereafter referred to as $SMH(i)$ —is calculated as the spatial standard deviation of the 25 values of S within the L_{evt} domain:

$$SMH = \sigma^{sp}(S_{Levt}) \quad (1)$$

To understand whether the location where precipitation occurs is relatively drier (or wetter) than its surroundings, we compute the inward soil moisture gradient (ISG) during the morning of the event day ($ISG(i)$), which is defined as the sum of the spatial “temporal evaporative stress anomalies” difference between L_{max} and the surrounding 24 pixels divided by the weight of their distances:

$$ISG = \sum_{k,h} \frac{S'_{L_{max}(x,y)} - S'_{(x+k,y+h)}}{\sqrt{k^2 + h^2}}, \text{ for } \begin{matrix} k \\ h \end{matrix} = -2, -1, 0, 1, 2, \quad (2)$$

where S' is the evaporative stress value having subtracted by the mean seasonal cycle, (x, y) is the position of L_{max} , and k (h) denotes the k th (h th) vertical (horizontal) grid next to L_{max} . As a result, an event with positive (negative) $ISG(i)$ denotes that precipitation occurs over soil anomalies that are relatively wetter (drier). The anomalous values (S') used here can mitigate the effects of fine-scale forcing in the following analysis of preferential precipitation locations. For particular soil moisture conditions of $SMH(i)$ and $S_{max}(i)$, we then compute R_{ISG} , the ratio of events with positive $ISG(i)$ to all events. The frequency of occurrence of precipitation on wetter (drier) soils than the surroundings is higher as R_{ISG} approaches 1 (0), and thus, R_{ISG} can be regarded as the “sign” and “strength” of the coupling. A two-tailed Z test is then used to examine whether the value of R_{ISG} is significantly different from the value of 0.5 that indicates no (or neutral) coupling.

Finally, we would like to distinguish between the words “coupling” and “feedback” in this study. The soil moisture-precipitation spatial (temporal) coupling is the spatial (temporal) preference of rain, which is

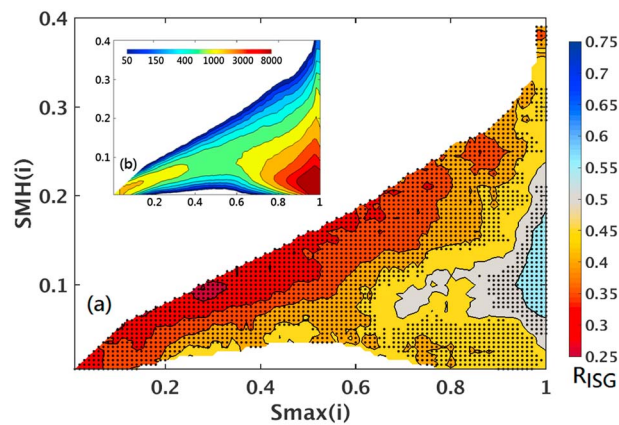


Figure 2. (a) Contours of R_{ISG} for the CMORPH-GLEAMc combination. Each R_{ISG} is calculated for specific ranges of soil wetness ($\pm 0.04 S_{max}(i)$) and SMH ($\pm 0.02 SMH(i)$) by each $0.01 S_{max}(i)$ and $0.01 SMH(i)$ interval. Number of events (N) with given soil moisture conditions less than 200 are left white. The black dots denote that the proportion (R_{ISG}) is significantly different from 0.5 at significance level of 0.05 based on the Z test under a null assumption that no preference exist ($R_{ISG} = 0.5$). (b) Number of events calculated for R_{ISG} . Results from various data set combinations are displayed in supporting information Figures S3 and S4.

$SMH(i)$ for the same $S_{max}(i)$ and increases with $S_{max}(i)$ for the same $SMH(i)$. This bottom right corner might indicate that very homogeneous soil moisture patterns are not able to influence the preferential location of precipitation. Also, it is worth mentioning that the signal can be impacted by different background climate factors or synoptic conditions, which are not considered in this study. Nonetheless, the overall pattern suggests that there is an increased preference for (a) negative spatial coupling when the soils are overall drier and the soil moisture heterogeneity is higher and (b) positive spatial coupling when the soil is overall wetter and close to the energy-limited regime of evapotranspiration. Therefore, wet soils and strong soil moisture heterogeneity are two competing effects in determining the location of afternoon precipitation. The results from different data set combinations agree on these general findings (supporting information Figure S3). Note that the large amount of samples in the bottom right corner cause small deviations from 0.5 to become significant.

Next, to further explore whether the behavior of R_{ISG} for specific soil moisture conditions is not simply a result of disparities between different regions of the globe, we cluster soil moisture conditions into nine groups based on the $S_{max}(i)$ and $SMH(i)$ shown in Figure 2. Given that each group should have similar R_{ISG} values, $S_{max}(i)$ and $SMH(i)$ are divided into unequal-sized intervals (see Figure 3 for details). We also provide maps with the number of events at a scale of 5° for each group to show how the signal in Figure 2 is affected by the spatial distribution (supporting information Figures S5–S7).

Figure 3 shows R_{ISG} globally at a scale of 5° for each group (see also supporting information Figures S8–S10). In each group, the preferences of precipitation location are rather consistent spatially, although small spatial variations of R_{ISG} do exist. Figure 3 also indicates that the negative spatial coupling is strongest in arid and semiarid regions. When $S_{max} > 0.9$ and moderately heterogeneous (SMH between 0.05 and 0.2), the probability of that precipitation that tends to occur on dry soils is significantly less than expected by chance. On the other hand, for the same regions, R_{ISG} can vary with different soil moisture conditions. For example, in semiarid regions, like the Sahel, where the soil conditions can cover a large range of soil wetness and heterogeneity, the sign of spatial coupling varies from negative to neutral (Figure 3, middle and bottom rows). Note that for the rightmost panel of Figure 3 (middle row), although R_{ISG} ostensibly deviates from 0.5 (approximately from 0.55 to 0.58) in some of these pixels, it is not statistically significant (i.e., $p > 0.05$) with tens of samples (events) (supporting information Figure S5).

Figure 4 summarizes the observed relationship: with sufficient soil moisture heterogeneity, the favored location of precipitation is different depending on soil wetness conditions. The possible mechanisms behind such relations are discussed in section 4.

identified through statistical analyses. The soil moisture-precipitation feedback is the physical loop whereby precipitation is influenced by soil moisture conditions from previous rain events.

3. Results

3.1. Preferred Precipitation Locations

Figure 2 displays how R_{ISG} varies with $S_{max}(i)$ and $SMH(i)$ globally. R_{ISG} significantly less (greater) than 0.5 shows more in drier (wetter) $S_{max}(i)$. This means relatively drier (wetter) patches have more possibilities to receive rain in dry (wet) conditions. On the other hand—except for the bottom right corner of Figure 2— R_{ISG} decreases with increasing

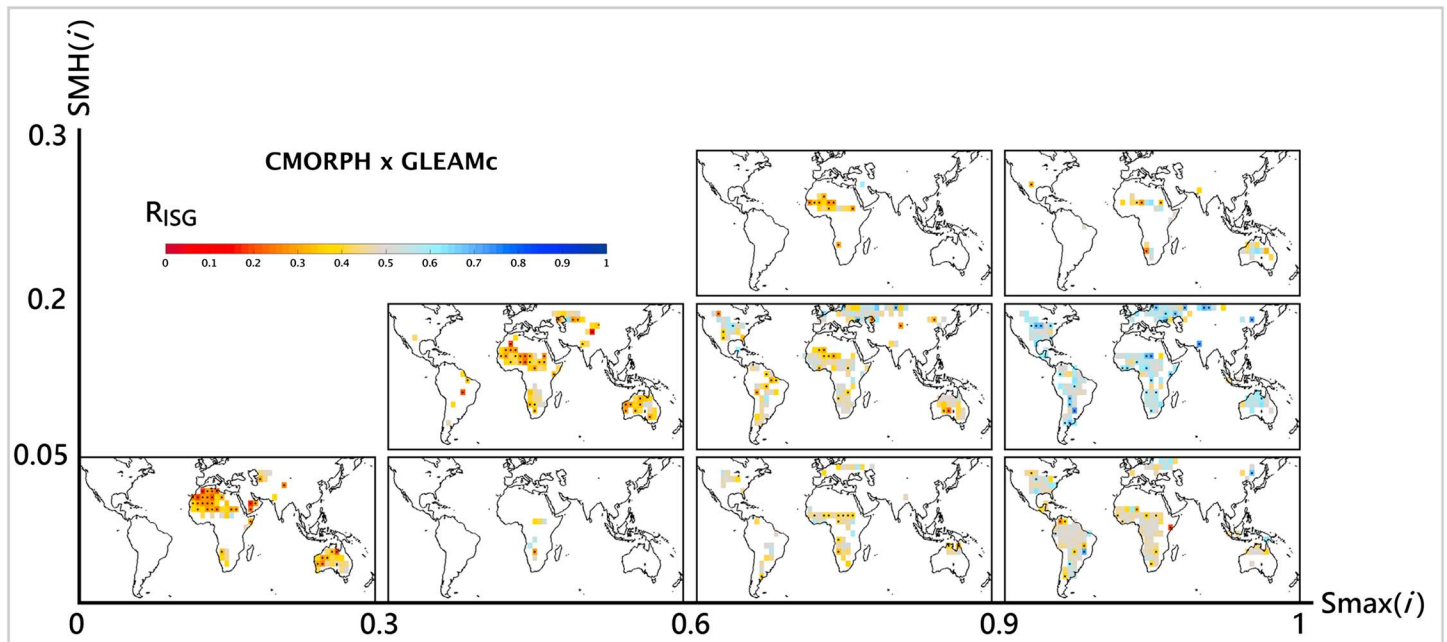


Figure 3. Maps of global R_{ISG} for specific soil moisture condition groups at a scale of 5° using the CMORPH-GLEAMc combination. S_{max} values are divided into four ranges (0–0.3, 0.3–0.6, 0.6–0.9, and 0.9–1), and SMH values are divided into three ranges (0–0.05, 0.05–0.2, and 0.2–0.3). Any grid box in which event number (N) < 25 is left white. The black dots denote that the proportion (R_{ISG}) is significantly different from 0.5 at the significance level of 0.05 based on the Z test. Results from various data set combinations are displayed in supporting information Figures S8–S10.

3.2. Effect of Precipitation Events on Next Day's Soil Moisture Conditions

Intuitively, for the 1 day cycle considered in this study, rain over spatially wetter (drier) soils should heterogenize (homogenize) the soil moisture pattern, and thus the positive (negative) spatial coupling ought to enhance (dampen) soil moisture spatial variability on the next day. To test this hypothesis, we explore how the spatial variability of soil moisture is altered by precipitation by calculating the difference in SMH before and after the precipitation event (referred to as dSMH and defined as $SMH(i+1)$ minus $SMH(i)$). The results are classified into nine groups (as in Figure 3, based on $S_{max}(i)$ and $SMH(i)$) and samples in each group are separated into two groups, one with positive and the other with negative values of $ISG(i)$, in order to examine whether it rains on wetter (drier) soils resulting in stronger (weaker) soil moisture heterogeneity. The statistical results for different soil moisture conditions are shown in Figure 5, in which the red and blue bins show the frequency of dSMH in the events with negative and positive $ISG(i)$, respectively. The proportion of positive dSMH to the entire population is displayed in the top right corner of each panel.

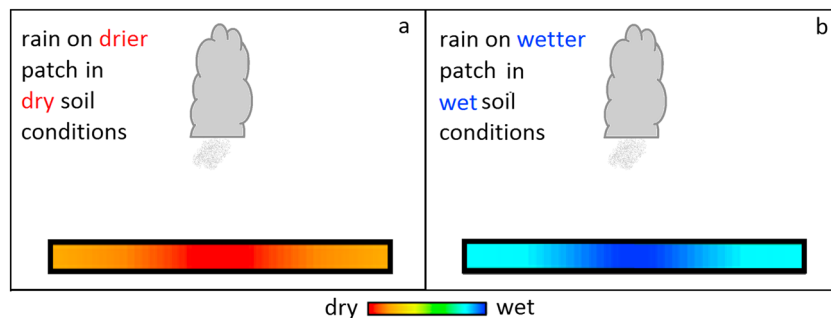


Figure 4. Schematic plots of the relationship between soil moisture heterogeneity, soil wetness, and precipitation location. The analysis of postrainfall soil moisture spatial pattern suggests that with equal and sufficient soil moisture heterogeneity, (a) rain is spatially more likely over dry soils in dry conditions and (b) rain is spatially more likely over wet soils in wet conditions.

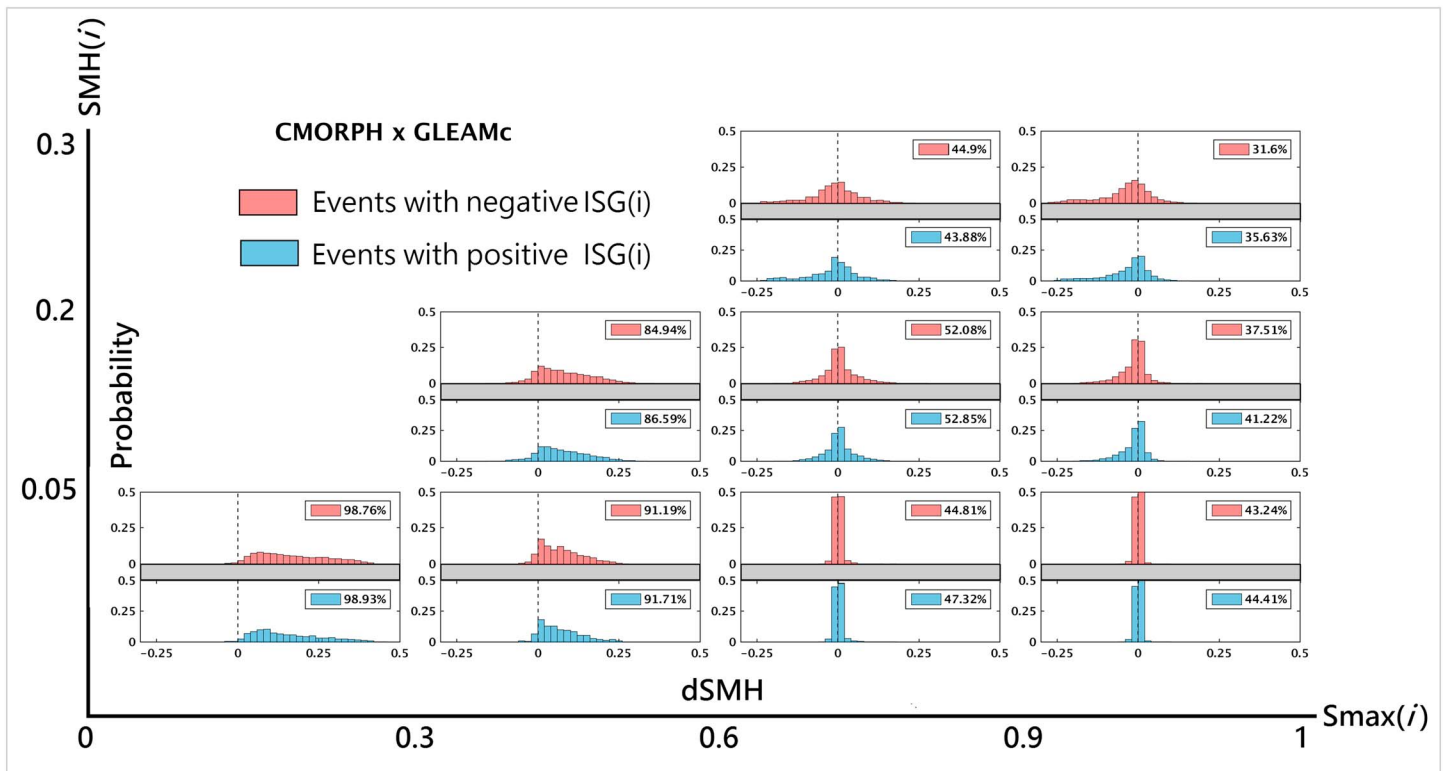


Figure 5. Histograms of the differences in soil moisture heterogeneity (dSMH) before and after precipitation events for the CMORPH-GLEAMc combination (red bins: events with negative ISG(i); blue bins: events with positive ISG(i)). The top right corner for each panel displays the proportion of positive dSMH events to the entire population (red: events with negative ISG(i); blue: events with positive ISG(i)). Results from various data sets combinations are displayed in supporting information Figures S11–S13.

In each group, whether it rains over relatively dry (red probability density function (pdf)) or wet (blue pdf) pixels, it has no significant effect on the ratio of positive dSMH. The ratio of positive dSMH decreases as soil conditions become wetter as shown in Figure 5 (see also supporting information Figures S11–S13). That is because the dry pixels become extremely wet after precipitation, while there is little or no precipitation in the surrounding regions, resulting in more heterogeneous conditions after precipitation events; this is especially the case when conditions are initially dry. Together with Figure 2, when soil conditions get drier, R_{ISG} gets smaller, but the ratio of positive dSMH gets larger. This reveals that spatial coupling tends to be negative in drier conditions but resulting in stronger soil moisture heterogeneity on the next day, which itself may increase the likelihood of further events, thereby indirectly contributing to a positive feedback on longer time scales.

Previous studies have indicated that the possibility of rain is higher when soil moisture conditions are wetter [Findell and Eltahir, 1997; Findell et al., 2011] and heterogeneous [Taylor et al., 2011; Guillod et al., 2015]. By combining these concepts with our results, this implies a possibility that the contribution of land to precipitation persistence would come not only from temporal soil wetness anomaly but also from soil moisture spatial heterogeneity: once a rain event occurs, it favors another event in the following days at the same location and its neighborhood. At the same location, this may be induced by the increasing soil wetness and evaporation, while at neighboring drier regions, it may be due to the enhanced soil moisture heterogeneity, and thus additional low-level atmospheric convergence.

4. Discussion

The above mentioned results are subject to several uncertainties. First, the data of evaporative stress from GLEAM may be prone to errors, especially in regions where satellite soil moisture observations are not available, like rainforests. In fact, a smaller part of the variability of S in GLEAM does not come from the soil

moisture but from the slow-varying observations of microwave vegetation optical depth (proxy for vegetation water content). As such, in regions for which the water content of vegetation is anomalously low with respect to its climatology, the evaporative stress increases (S decreases), even if enough soil moisture is present in the soil [Martens *et al.*, 2016]. This is intended to improve the representation of phenological processes and occasional disturbances that lead to a change in the soil moisture–evaporation relationship—e.g., deciduous forest during leaf-out or cropland regions after harvesting. Thus, while most of the variability in S responds to soil moisture in rainforests, if the vegetation water content is anomalously low in the wet season, the S in GLEAM will be lowered and that effect will be propagated to the transpiration. The realism of model transpiration estimates in rainforests is extremely hard to assess, because of the difficulties to obtain reliable field measurements and the problems to disentangle the impact of rainfall interception. Nonetheless, we further conduct the supporting information Figure S14 to show that the findings are not sensitive to the exclusion of tropical regions from the analysis.

Second, we use anomalous evaporative stress for the analysis to mitigate the influence of both topographic forcing on convection and larger-scale climatological gradients of rainfall, since in these two cases the location which receives more rain is likely to exhibit higher climatological values of S even without any soil moisture–precipitation feedback. However, using anomalous evaporative stress (S') could simultaneously eliminate the possibly positive feedback in the signal—in climatically wetter region, rain occurs more often because it is wetter than surroundings; thus, the coupling signal (values of R_{ISG}) could be slightly underestimated by using S' in the analysis. To examine the sensitivity of using S and S' on the signal, results using total evaporative stress (S) are provided in supporting information Figures S15b and S16a, of which R_{ISG} values are overall slightly greater, compared to results using S' .

Despite many concerns, results with slightly adjusted method show similar patterns (Figures S14–S16). Therefore, rather than identifying the sign of spatial coupling in specific soil wetness and heterogeneity (the R_{ISG} values in specific soil moisture conditions), we emphasize that the preferential precipitation locations are dependent on different soil moisture patterns (the changes in R_{ISG} at various soil moisture conditions). An element that our analysis does not explicitly analyze is the effect of background wind, which was shown to affect the spatial sign of soil moisture–precipitation feedback via supporting the convective cells to propagate [Froidevaux *et al.*, 2014]. Finally, one should keep in mind that large parts of the continental surface are not included in the analysis due to potential confounding effects from topography or water bodies (Figure 1a).

Analysis of the soil moisture spatial distribution prior to precipitation events highlights a negative (positive) spatial coupling in dry (extremely wet) soil moisture conditions. In addition, negative spatial coupling is stronger in dry and heterogeneous soil moisture conditions, which are frequently found in arid and semiarid regions. This is somewhat consistent with Taylor *et al.* [2012] and Guillod *et al.* [2015] in that the negative spatial coupling appears more clearly over semiarid regions. Separate studies have shown that strong soil moisture heterogeneity [Taylor *et al.*, 2011] and wet average conditions [Eltahir, 1998] both favor the development of convection. This study suggests a different but compatible relation: the soil moisture heterogeneity and soil wetness conditions collaboratively affect the precipitation position and thus play a role in mesoscale moisture recycling. Assuming that this relation between preferential precipitation location and antecedent soil moisture is deterministic, our results suggest the coexistence of positive and negative soil moisture–precipitation spatial feedback mechanisms and a competition between them for the dominance in a given soil moisture pattern.

In the positive mechanisms, the wetter soil (compared to the surrounding) results in a larger moist entropy flux into the boundary layer [Schär *et al.*, 1999], resulting in higher relative humidity in the lower atmosphere and thereby potentially building shallow boundary layers. This leads to enhanced moist static energy per unit mass of the boundary layer air [Eltahir, 1998] over wetter patches and thus enhances the atmospheric instability (positive effect). In the negative mechanisms, the soil moisture heterogeneity provides an external forcing (via lower level water vapor convergence) and creates an ascending motion to enhance the atmospheric instability over the drier patches (negative effect). Therefore, for equal and sufficient soil moisture heterogeneity, soil wetness can also influence the location of precipitation—over the wet soils in a heterogeneous landscape, the positive effect outweighs the negative effect, and thus, precipitation more likely occurs over wetter patches (as in Figure 4b), and the opposite occurs for dry soils (as in Figure 4a).

The results with spatial average of S as a measure of soil wetness (instead of S_{\max}) are provided in the supporting information Figures S15c and S16b, which show different pattern with Figure 2a but convey the same message. Note that for two soil moisture patterns with the same average wetness, the one with stronger heterogeneity also contains a wetter pixel than the other, and thus, both negative effect and positive effect could be stronger.

Another important contribution of this study is the analysis of postprecipitation soil moisture patterns, which shows that precipitation events can increase the short-term soil moisture spatial variability depending on the original soil moisture conditions. In dry conditions, precipitation tends to make the soil moisture spatial pattern more heterogeneous, indicating that both positive (soil wetness increases) and negative (soil moisture heterogeneity increases) soil moisture-precipitation feedback mechanisms would be stronger over the altered soil moisture pattern and thus might further enhance precipitation persistence. This result supports the hypothesis by Taylor *et al.* [2011] that the modifications to soil moisture patterns by precipitation events favor another mesoscale convective system in the days following the initial event. A similar conclusion was drawn in the earlier regional model study [Emori, 1998], stating that the intense precipitation occurs preferably over drier surfaces, which leads to a spontaneously development of horizontal soil moisture contrasts and thus maintains the heterogeneity in soil moisture; such spatial characteristic of precipitation location and altered soil moisture distribution is more obvious in initially dry conditions. This raises the question to what extent the soil moisture pattern plays a role in precipitation persistence. Recent work based on observations at 0.25° spatial scales by Tuttle and Salvucci [2016] also showed that temporal soil moisture anomalies can influence the probability of precipitation. In addition to soil wetness and atmospheric conditions, whether spatial variability in soil moisture can enhance precipitation persistence is worth further investigation.

5. Conclusion

Generally, through evapotranspiration, the impact of soil moisture on lower atmospheric temperature is negative [Cheruy *et al.*, 2013; Lo and Famiglietti, 2013]. However, the feedbacks of soil moisture on precipitation are far less straightforward: they can be either positive or negative, depending on local atmospheric stability and the larger-scale atmospheric circulation. In this study of 10 years of precipitation and evaporative stress, we characterize precipitation location in relation to soil wetness conditions and the mesoscale soil moisture heterogeneity. Results show that (a) afternoon rainfall is more frequent over drier patches during dry times, but more frequent over wet patches during extremely wet times; (b) soil moisture heterogeneity intensifies negative coupling and buffers positive coupling; and (c) negative spatial coupling tends to enhance the soil moisture heterogeneity rather than leading to homogeneously wetter soils on the following day. The observed relations explored here between precipitation location and antecedent/subsequent soil moisture provide a new view of soil moisture-precipitation coupling, which can be further examined via numerical model experiments (such as in Wu *et al.* [2015]). To better represent such relationships in climate models, identifying the physical pathways behind them will be required.

Acknowledgments

We are grateful to Yuying Zhang for the discussion. This study was supported by the MOST 105-2111-M-002-003 to National Taiwan University. D.G. Miralles acknowledges support from the European Research Council (ERC) under grant agreement 715254 (DRY-2-DRY). The data sets used in this study are listed in the references.

References

- Amante, C., and B. W. Eakins (2009), Etopo1 1 arc-minute global relief model: Procedures, data sources and analysis, *NOAA Tech. Memo. NESDIS NGDC*, 24, 1–19, doi:10.7289/V5C8276M.
- Bartholomé, E., and A. S. Belward (2005), GLC2000: A new approach to global land cover mapping from Earth observation data, *Int. J. Remote Sens.*, 26(9), 1959–1977, doi:10.1080/01431160412331291297.
- Berg, A., K. Findell, B. R. Lintner, P. Gentile, and C. Kerr (2013), Precipitation sensitivity to surface heat fluxes over North America in reanalysis and model data, *J. Hydrometeorol.*, 14(3), 722–743.
- Brubaker, K. L., D. Enthekebi, and P. S. Eagleson (1993), Estimation of continental precipitation recycling, *J. Clim.*, 6, 1077–1089, doi:10.1029/95JD02135.
- Cheruy, F., *et al.* (2013), Combined influence of atmospheric physics and soil hydrology on the simulated meteorology at the SIRTa atmospheric observatory, *Clim. Dyn.*, 40, 2251–2269, doi:10.1007/s00382-012-1469-y.
- Dee, D. P., *et al.* (2011), The ERA-Interim reanalysis: Configuration and performance of the data assimilation system, *Q. J. R. Meteorol. Soc.*, 137, 553–597, doi:10.1002/qj.828.
- Dirmeyer, P. A., *et al.* (2012), Evidence for enhanced land-atmosphere feedback in a warming climate, *J. Hydrometeorol.*, 13, 981–995.
- D'Odorico, P., and A. Porporato (2004), Preferential states in soil moisture and climate dynamics, *Proc. Nat. Acad. Sci. U.S.A.*, 101(24), 8848–8851, doi:10.1073/pnas.0401428101.
- Eltahir, E. A. B. (1998), A soil moisture–rainfall feedback mechanism: 1. Theory and observations, *Water Resour. Res.*, 34, 765–776, doi:10.1029/97WR03499.
- Eltahir, E. A. B., and R. L. Bras (1996), Precipitation recycling, *Rev. Geophys.*, 34, 367–378, doi:10.1029/96RG01927.

- Emori, S. (1998), The interaction of cumulus convection with soil moisture distribution: An idealized simulation, *J. Geophys. Res.*, *103*, 8873–8884, doi:10.1029/98JD00426.
- Findell, K. L., and E. A. B. Eltahir (1997), An analysis of the soil moisture-rainfall feedback, based on direct observations from Illinois, *Water Resour. Res.*, *33*, 725–735, doi:10.1029/96WR03756.
- Findell, K. L., and E. A. B. Eltahir (2003), Atmospheric controls on soil moisture boundary layer interactions, part I, Framework development, *J. Hydrometeorol.*, *4*, 552–569, doi:10.1175/1525-7541(2003)004<0552:ACOSML>2.0.CO;2.
- Findell, K. L., P. Gentile, B. R. Lintner, and C. Kerr (2011), Probability of afternoon precipitation in eastern United States and Mexico enhanced by high evaporation, *Nat. Geosci.*, *4*(7), 434–439, doi:10.1038/ngeo1174.
- Ford, T. W., A. D. Rapp, and S. M. Quiring (2015), Does afternoon precipitation occur preferentially over dry or wet soils in Oklahoma?, *J. Hydrometeorol.*, *16*, 874–888, doi:10.1175/JHM-D-14-0005.1.
- Froidevaux, P., L. Schlemmer, J. Schmidli, W. Langhans, and C. Schär (2014), Influence of the background wind on the local soil moisture-precipitation feedback, *J. Atmos. Sci.*, *71*(2), 782–799, doi:10.1175/JAS-D-13-0180.1.
- Guillod, B. P., et al. (2014), Land-surface controls on afternoon precipitation diagnosed from observational data: Uncertainties and confounding factors, *Atmos. Chem. Phys.*, *14*, 8343–8367, doi:10.5194/acp-14-8343-2014.
- Guillod, B. P., et al. (2015), Reconciling spatial and temporal soil moisture effects on afternoon rainfall, *Nat. Commun.*, *6*, doi:10.1038/ncomms7443.
- Harper, A., I. T. Baker, A. S. Denning, D. A. Randall, D. Dazlich, and M. Branson (2014), Impact of evapotranspiration on dry season climate in the Amazon forest, *J. Clim.*, *27*, 574–591, doi:10.1175/JCLI-D-13-00074.1.
- Hsu, K.-L., X. Gao, S. Sorooshian, and H. V. Gupta (1997), Precipitation estimation from remotely sensed information using artificial neural networks, *J. Appl. Meteorol.*, *36*, 1176–1190, doi:10.1175/1520-0450(1997)036<1176:PEFRSI>2.0.CO;2.
- Huffman, G. J., et al. (2007), The TRMM multisatellite precipitation analysis (TMPA): Quasi-global, multiyear, combined-sensor precipitation estimates at fine scales, *J. Hydrometeorol.*, *8*, 38–55, doi:10.1175/JHM560.1.
- Joyce, R. J., J. E. Janowiak, P. A. Arkin, and P. Xie (2004), CMORPH: A method that produces global precipitation estimates from passive microwave and infrared data at high spatial and temporal resolution, *J. Hydrometeorol.*, *5*, 487–503, doi:10.1175/1525-7541(2004)005<0487:CAMTPG>2.0.CO;2.
- Koster, R. D., et al. (2004), Regions of strong coupling between soil moisture and precipitation, *Science*, *305*, 1138–1140, doi:10.1126/science.1100217.
- Lin, Y.-H., M.-H. Lo, and C. Chou (2016), Potential negative effects of groundwater dynamics on dry season convection in the Amazon River basin, *Clim. Dyn.*, *46*, 1001–1003, doi:10.1007/s00382-015-2628-8.
- Lo, M.-H., and J. S. Famiglietti (2013), Irrigation in California's Central Valley strengthens the southwestern U.S. water cycle, *Geophys. Res. Lett.*, *40*, 301–306, doi:10.1002/grl.50108.
- Martens, B., D. G. Miralles, H. Lievens, R. van der Schalie, R. A. M. de Jeu, D. Fernández-Prieto, H. E. Beck, W. A. Dorigo, and N. E. C. Verhoest (2016), GLEAM v3: Satellite-based land evaporation and root-zone soil moisture, *Geosci. Model Dev. Discuss.*, doi:10.5194/gmd-2016-162.
- Miralles, D. G., T. R. H. Holmes, R. A. M. de Jeu, J. H. Gash, A. G. C. A. Meesters, and A. J. Dolman (2011), Global land-surface evaporation estimated from satellite-based observations, *Hydrol. Earth Syst. Sci.*, *15*, 453–469, doi:10.5194/hess-15-453-2011, in review.
- Miralles, D. G., A. J. Teuling, C. C. van Heerwaarden, and J. V.-G. de Arellano (2014), Mega-heatwave temperatures due to combined soil desiccation and atmospheric heat accumulation, *Nat. Geosci.*, *7*(5), 345–349, doi:10.1038/NGEO2141.
- Ookouchi, Y., M. Segal, R. C. Kessler, and R. A. Pielke (1984), Evaluation of soil moisture effects on the generation and modification of mesoscale circulations, *Mon. Weather Rev.*, *112*, 2281–2292, doi:10.1175/1520-0493(1984)112<2281:EOSMEO>2.0.CO;2.
- Owe, M., R. de Jeu, and T. Holmes (2008), Multisensor historical climatology of satellite-derived global land surface moisture, *J. Geophys. Res.*, *113*, F01002, doi:10.1029/2007JF000769.
- Schär, C., D. Lüthi, U. Beyerle, and E. Heise (1999), The soil-precipitation feedback: A process study with a regional climate model, *J. Clim.*, *12*, 722–741.
- Seneviratne, S. I., T. Corti, E. L. Davin, M. Hirschi, E. B. Jaeger, I. Lehner, B. Orlowsky, and A. J. Teuling (2010), Investigating soil moisture-climate interactions in a changing climate: A review, *Earth-Sci. Rev.*, *99*(3–4), 125–161, doi:10.1016/j.earscirev.2010.02.004.
- Taylor, C. M. (2015), Detecting soil moisture impacts on convective initiation in Europe, *Geophys. Res. Lett.*, *42*, 4631–4638, doi:10.1002/2015GL064030.
- Taylor, C. M., and T. Lebel (1998), Observational evidence of persistent convective-scale rainfall patterns, *Mon. Weather Rev.*, *126*, 1597–1607, doi:10.1175/1520-0493(1998)126<1597:OEOPCS>2.0.CO;2.
- Taylor, C. M., A. Gounou, F. Guichard, P. P. Harris, R. J. Ellis, F. Couvreur, and M. De Kauwe (2011), Frequency of Sahelian storm initiation enhanced over mesoscale soil-moisture patterns, *Nat. Geosci.*, *4*, 430–433, doi:10.1038/ngeo1173.
- Taylor, C. M., R. A. M. de Jeu, F. Guichard, P. P. Harris, and W. A. Dorigo (2012), Afternoon rain more likely over drier soils, *Nature*, *489*, 423–426, doi:10.1038/nature11377.
- Tuttle, S., and G. Salvucci (2016), Empirical evidence of contrasting soil moisture-precipitation feedbacks across the United States, *Science*, *352*, 825–828, doi:10.1126/science.aaa7185.
- Wielicki, B. A., B. R. Barkstrom, E. F. Harrison, R. B. Lee III, G. L. Smith, and J. E. Cooper (1996), Clouds and the Earth's Radiant Energy System (CERES): An Earth observing system experiment, *Bull. Am. Meteorol. Soc.*, *77*, 853–868, doi:10.1175/1520-0477(1996)077<0853:CATERE>2.0.CO;2.
- Wu, C.-M., M.-H. Lo, W.-T. Chen, and C.-T. Lu (2015), The impacts of heterogeneous land surface fluxes on the diurnal cycle precipitation: A framework for improving the GCM representation of land-atmosphere interactions, *J. Geophys. Res. Atmos.*, *120*, 3714–3727, doi:10.1002/2014JD023030.
- Yang, S., and E. A. Smith (2008), Convective-stratiform precipitation variability at seasonal scale from 8 yr of TRMM observations: Implications for multiple modes of diurnal variability, *J. Clim.*, *21*, 4087–4114, doi:10.1175/2008JCLI2096.1.
- Zhou, Y., D. Wu, W. Lau, and W. Tao (2016), Scale dependence of land atmospheric interactions in wet and dry regions as simulated with NU-WRF over southwest and South-Central US, *J. Hydrometeorol.*, *17*, 2121–2136, doi:10.1175/JHM-D-16-0024.1.